Electrical isolation of InGaP by proton and helium ion irradiation

I. Danilov, J. P. de Souza, H. Boudinov, J. Bettini, and M. M. G. de Carvalho

Citation: Journal of Applied Physics **92**, 4261 (2002); doi: 10.1063/1.1506200
View online: http://dx.doi.org/10.1063/1.1506200
View Table of Contents: http://scitation.aip.org/content/aip/journal/jap/92/8?ver=pdfcov
Published by the AIP Publishing

Electrical isolation of InGaP by proton and helium ion irradiation

I. Danilov, J. P. de Souza, and H. Boudinov[a)]
Instituto de Física, UFRGS, 91501-970 Porto Alegre, RS, Brazil

J. Bettini and M. M. G. de Carvalho
Instituto de Física "Gleb Wataghin," UNICAMP, 13083-970 Campinas, SP, Brazil

(Received 12 February 2002; accepted for publication 16 July 2002)

Formation of electrical isolation in *n*- and *p*-type $In_{0.49}Ga_{0.51}P$ epitaxial layers grown on semi-insulating GaAs substrates was investigated using proton or helium ion irradiation. Sheet resistance increases with the irradiation dose, reaching a saturation level of $\approx 10^9\ \Omega/\square$. The results show that the threshold dose necessary for complete isolation linearly depends on the original carrier concentration either in *p*- or *n*-type doped InGaP layers. Thermal stability of the isolation during postirradiation annealing was found to increase with accumulation of the ion dose. The maximum temperature at which the isolation persists is $\cong 500\,^{\circ}C$. © *2002 American Institute of Physics.* [DOI: 10.1063/1.1506200]

I. INTRODUCTION

Structures consisting of an epitaxial $In_{0.49}Ga_{0.51}P$ layer grown matched on GaAs are promising for the fabrication of microelectronic and optoelectronic devices, such as heterojunction bipolar transistors (HBTs) with wide-band-gap emitters[1] and laser structures composed by InGaP/GaAs confining layers and InGaAs quantum well active regions.[2]

An important subject, which is related to fabrication of devices using such structures, is electrical isolation. For example, it is necessary to prepare highly resistive regions for electrical separation of individual devices on the semi-insulating GaAs substrate. Mesa etching[3] of InGaP conductive layers is the simplest method to obtain isolation. However, in order to attain highly resistive isolated regions the etching is usually deep, leading to a lack of planarity in the structures, which may cause device failure associated with the breaking of metal connections. Additionally, a deep etched layer in laser structures causes discontinuity of the effective refractive index in GaAs waveguides.

Electrical isolation of III–V semiconductors formed by introduction of a controlled concentration of point defects from light ion irradiation is a well-established technique.[4] Besides the efficiency of this method to obtain highly isolated layers, it has the additional advantage of keeping the planarity of the isolated structures.

Highly resistive regions can be produced by irradiation of *n*- and *p*-type InGaP layers using light mass ions.[5–8] Some trends can be noted in the published data, which are similar to that observed in irradiated GaAs.[9] For example, the dose required to obtain maximum sheet resistance (threshold dose for complete isolation, D_{th}) in InGaP decreases with increasing of ion mass [from $1\times10^{14}\ cm^{-2}$ for He^+ ions (Ref. 6) to $5\times10^{12}\ cm^{-2}$ for B^+ ions (Ref. 5)], and the sheet resistance (R_s) decreases with hopping conduction after irradiation with doses well above D_{th}.[6,7] However, it is difficult to make a comparative analysis of the results from previous reports,[5–8] because they employed carrier concentrations in a narrow range ($0.1–1.1\times10^{18}\ cm^{-3}$ for *n*-type samples and $1.0–4.2\times10^{18}\ cm^{-3}$ for *p*-type samples), InGaP layers of different thickness, and ions of different mass and energy.

During a postirradiation annealing the formed isolation in irradiated InGaP was observed to persist up to temperatures in the range of 400–600 °C.[6,7] However, factors that determine the thermal behavior of R_s in irradiated InGaP layers and the dependence of D_{th} on the original carrier concentration in the InGaP layers were not presented in the publications.

Although ion irradiation has been used for the formation of highly resistive regions in InGaP wide-band-gap emitters of HBTs,[10,11] a deeper understanding of this method is urged to extend its application to other devices, such as, for example, Al-free heterostructure quantum well lasers with InGaP cladding layers.

In the present article, a systematic investigation on the dependence of the threshold dose for isolation with the donor or acceptor original concentration in InGaP/GaAs structures and their thermal stability is reported.

II. EXPERIMENTAL DETAILS

The InGaP layers were grown on semi-insulating GaAs substrates of (100) orientation using chemical beam epitaxy in a Riber 32 system. Before the epitaxial growth, the surface oxide was desorbed at 590 °C during 20 min under AsH_3 flow. The doped $In_{0.49}Ga_{0.51}P$ layers were epitaxially grown on a 0.3 μm undoped GaAs buffer layer at the temperature of 540 °C (*n*-type) or 500 °C (*p*-type) with a growth rate of $\cong 1\ \mu$m/h. Solid silicon or beryllium was evaporated from effusion cells at temperatures in the range of 1050–1200 or 700–850 °C, respectively, for *n*- and *p*-type doping. Details of the electrical properties and crystal structure of the InGaP layers produced using the present method have been described elsewhere.[12]

[a)]Electronic mail: henry@if.ufrgs.br

Wafers of three different structures were prepared and named as A, B, and C. Structure A contains a 0.85-μm-thick InGaP p-type layer with hole concentration (p_0) of 1×10^{18} cm^{-3}. Structure B comprises a n-type 0.8-μm-thick InGaP layer with electron concentration (n_0) in the range from 5×10^{16} to 1.2×10^{19} cm^{-3}. Structure C contains a p-type 0.4-μm-thick InGaP layer with hole concentration in the range from 3.1×10^{17} to 1.8×10^{19} cm^{-3}. The wafers were cleaved in pieces to obtain rectangular resistors of 3×6 mm^2. For the Ohmic contacts to the p-type resistors In–Zn(2%), strips of $\cong3\times0.5$ mm^2 of area were manually applied on the InGaP surface, close to the 3 mm borders of the sample. In the case of n-type resistors, a similar procedure using In was adopted. The contacts were alloyed at 450 °C for 5 min in N_2 flow. The In or In–Zn(2%) contact layers provided a mask, which protected the underneath region from the ion irradiation.

The ion energies were chosen based on simulated damage profiles using the TRIM code.[13] Displacement energies of 7, 9, and 9 eV were assumed in the simulations, respectively, for In, Ga, and P.[14] The ion irradiation steps were performed with the samples kept at nominal room temperature, using ion current density in the range of 0.005–0.3 μA/cm^2. In order to minimize channeling effects, the sample surface normal was tilted 7° with respect to the beam incidence direction and rotated 25° with respect to the ⟨110⟩ direction.

The R_s values were measured after each dose step using a Keithley 617 electrometer without breaking the vacuum in the target chamber. The resistors used in the postirradiation annealing study were irradiated to a single dose step. The postirradiation annealing cycles were performed in argon atmosphere, using a halogen lamp rapid thermal annealing furnace. The annealing cycles employed a heating rate of 50 °C/s and time duration of 60 s.

III. RESULTS AND DISCUSSION

Figure 1 shows the evolution of R_s in a p-type resistor of structure A during proton irradiation at the energy of 240 keV. The evolution of R_s in the InGaP resistor proceeded quite similarly to the ones previously observed in the GaAs (Ref. 15) and InP resistors.[16] For doses below 1×10^{14} cm^{-2}, R_s remains practically constant at the value of $\approx2\times10^4$ Ω/□. However, in the dose range of 1.5–2.5×10^{14} cm^{-2}, R_s sharply increases by about four orders of magnitude. The increase of R_s should be attributed to carrier trapping at the irradiation damage centers and degradation of carrier mobility in the InGaP layer. For this sample, a dose of 2.5×10^{14} cm^{-2} corresponds to the isolation threshold dose. It is expected that for doses $\geqslant D_{\text{th}}$ all the carries in the InGaP layer have been trapped already. This explains the formation of a plateau in the curve, extending from a dose of 2.5×10^{14} to 5×10^{14} cm^{-2}. The R_s value ($\approx10^9$ Ω/□) in the plateau is determined by parallel conduction paths through the undoped GaAs buffer layer and the SI–GaAs substrate. For doses $\geqslant5\times10^{14}$ cm^{-2} the damage concentration becomes high enough to permit carrier transport via hopping conduction, causing a decrease of R_s.

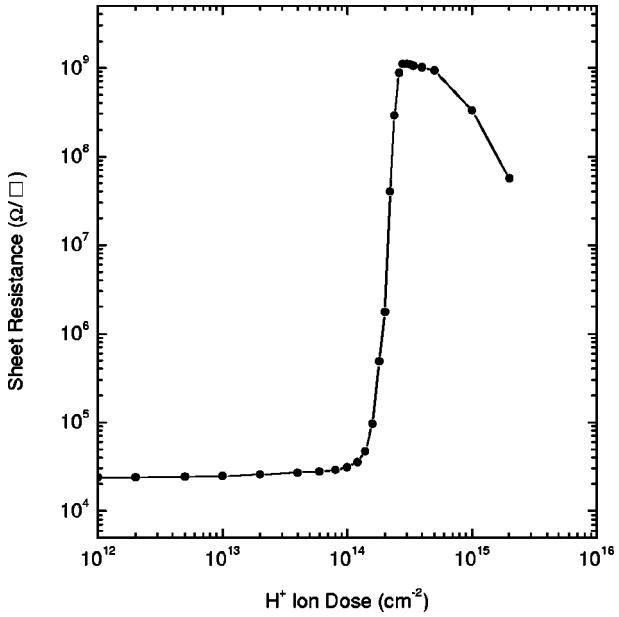

FIG. 1. Evolution of the sheet resistance in a p-type InGaP resistor of structure A during irradiation with protons at the energy of 240 keV.

Figure 2 shows the evolution of R_s in resistors of structure B during irradiation with He ions at the energy of 270 keV. Curves (1)–(4) were obtained from samples with n_0 of 4.8×10^{16}, 6.1×10^{17}, 2.1×10^{18}, and 1.2×10^{19} cm^{-3}, respectively. One can note the shift of D_{th} toward higher values with the increase of the original carrier concentration. This phenomenon will be discussed later in the text. Another interesting peculiarity is the close match of all the curves in the region where the resistivity is dominated by hopping conduction. It can be understood considering that in all samples the

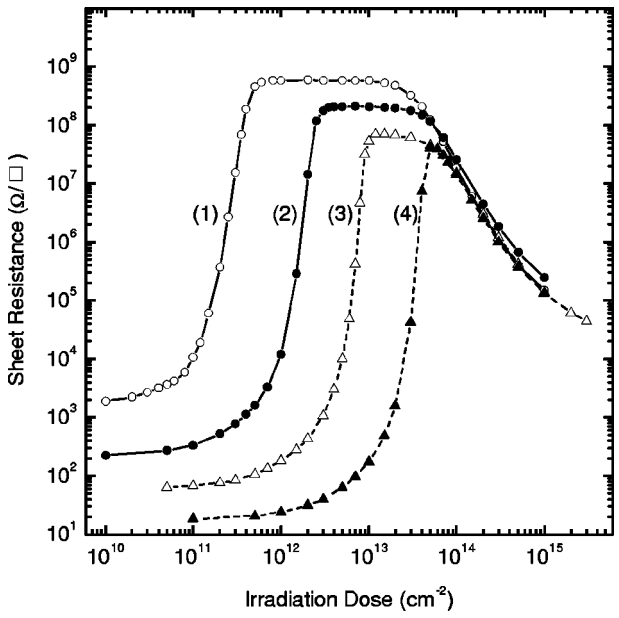

FIG. 2. Evolution of the sheet resistance in n-type InGaP resistors of structure B during irradiation with He ions at the energy of 270 keV. The original electron concentrations in the resistors are 4.8×10^{16} cm^{-2}, and 6.1×10^{17}, 2.8×10^{18}, and 1.2×10^{19} cm^{-3}, respectively, for the curves (1), (2), (3), and (4).

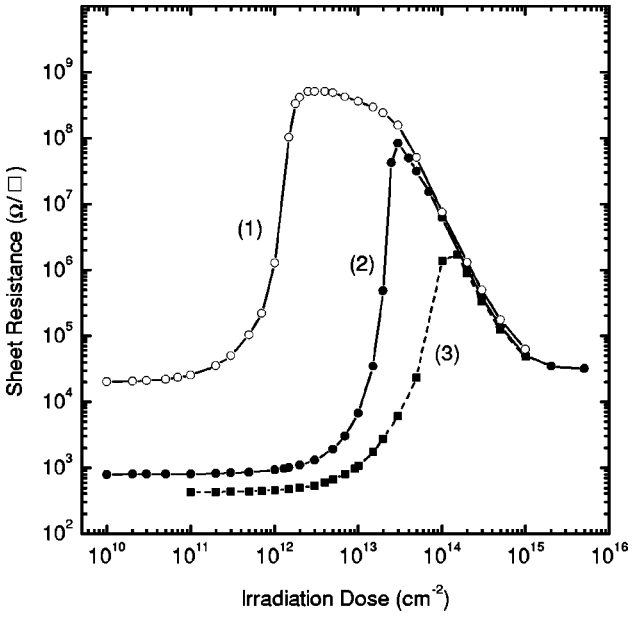

FIG. 3. Evolution of the sheet resistance in *p*-type InGaP resistors of structure C during irradiation with He ions at the energy of 270 keV. The original hole concentrations in the resistors are 3.1×10^{17}, 5.4×10^{18}, and 1.8×10^{19} cm^{-3}, respectively, for curves (1), (2), and (3).

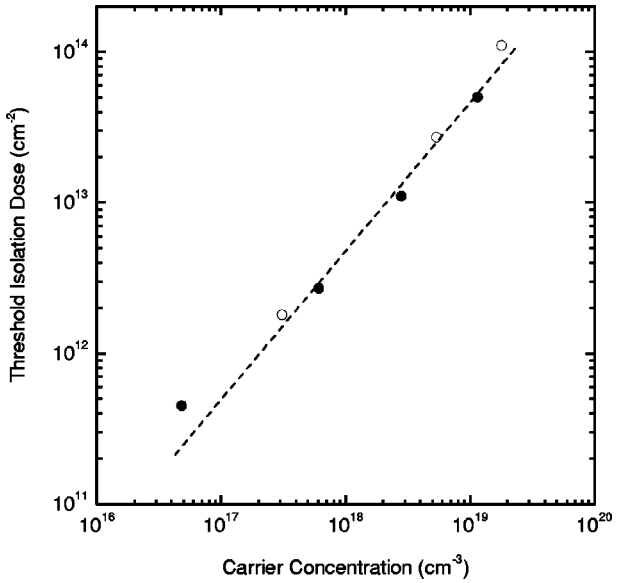

FIG. 4. Experimental values of the threshold isolation dose versus the original carrier concentration in *p*-type (open circles) and *n*-type (closed circles) InGaP resistors for He ion irradiation at the energy of 270 keV.

hopping conduction takes place in the GaAs substrate material where the peak of the damage concentration depth profile is located. The monotonic decrease of R_s value in the plateaus with the increase of n_0 is a phenomenon for which we do not have a plausible explanation at this moment. Further work needs to be undertaken in order to clarify this point.

The evolution of R_s in *p*-type resistors (of structure C) during He ion irradiation is presented in Fig. 3 for p_0 values of 3.1×10^{17} [curve (1)], 5.4×10^{18} cm^{-3} [curve (2)], and 1.8×10^{19} cm^{-3} [curve (3)].

Similarly to what was observed in *n*-type resistors (see Fig. 2), curve (1) of Fig. 3 presents the three distinct regions as discussed above. However, in curves (2) and (3) of Fig. 3 the plateaus are absent. It can be explained considering the heavy doping level of these samples, for which the corresponding D_{th} values are higher than the onset dose for hopping conduction in the underneath GaAs damage layer.

The D_{th} values obtained from the data in Figs. 2 and 3, respectively, for *n*- and *p*-type resistors, are plotted versus the original carrier concentration (n_0 or p_0) in Fig. 4. A unique linear relationship was found that fits closely the data points obtained from both *n*- and *p*-type InGaP layers. It indicates that there is a direct proportion of the carrier concentration and the required minimum damage concentration to capture all carriers.

Considering that the observed behavior of R_s during dose accumulation is quite similar to those observed in GaAs (Ref. 15) and InP,[16] it is plausible to presume that the carrier trapping in the InGaP material is also performed by antisite defects (P_{Ga}, P_{In}, Ga_P, and In_P) and/or their related defect complexes created in the replacement collisions. For the *n*-type (*p*-type) InGaP the Ga_P and In_P (P_{In} and P_{Ga}) antisite defects and/or antisite related defect complexes should compose the electron (hole) traps. From the data in Fig. 4 one can infer that for each single 270 keV He ion about $\approx1.5-2.0\times10^5$ carriers are removed per cm along the depth in the InGaP layer. On the other hand, according to TRIM (Ref. 13) code simulation, each single 270 keV He ion produces $\approx3\times10^5-4\times10^5$ replacement collisions per cm. Consequently, $\cong2\pm0.5$ replacement collisions are necessary for the capture of each single carrier in the InGaP material. It should be pointed out that this estimate is rather rough because the damage distribution is not constant along the depth of the InGaP layer.

The obtained number of $\cong2\pm0.5$ replacement collisions per carrier captured fits reasonably well the one that we would expect according to the following reasoning. In III–V compound semiconductors of similar displacement energies, 25% of all replacement collisions result in V_{III} antisite defects and 25% in III_V antisite defects. By another side, the V_{III} (III_V) antisite defect is a double hole (double electron) trap. Consequently, the ratio of replacement collisions and captured carrier should be 2, which reasonably agrees with the observed number ($\cong2\pm0.5$).

The estimate number of replacement collisions per captured carrier can be useful when D_{th} from irradiation runs involving ions of different masses and energies need to be compared. For example, according to TRIM (Ref. 13) code simulation irradiation with 240 keV protons produces a replacement concentration in the InGaP layer ≈35 times lower than that of 270 keV He ions, at the same dose. Taking from Fig. 4 the D_{th} value corresponding to a carrier concentration of 1×10^{18} cm^{-3} for structure A and multiplying it by 35 one obtains $\cong2.1\times10^{14}$ cm^{-2}. This estimated D_{th} value agrees satisfactorily with the experimental one of $\cong2.5\times10^{14}$ cm^{-2} (see Fig. 1).

An important issue concerning application of the ion irradiation process to device fabrication technology is the thermal stability of the isolation during postirradiation annealing. In the present study the thermal stability in structures A,

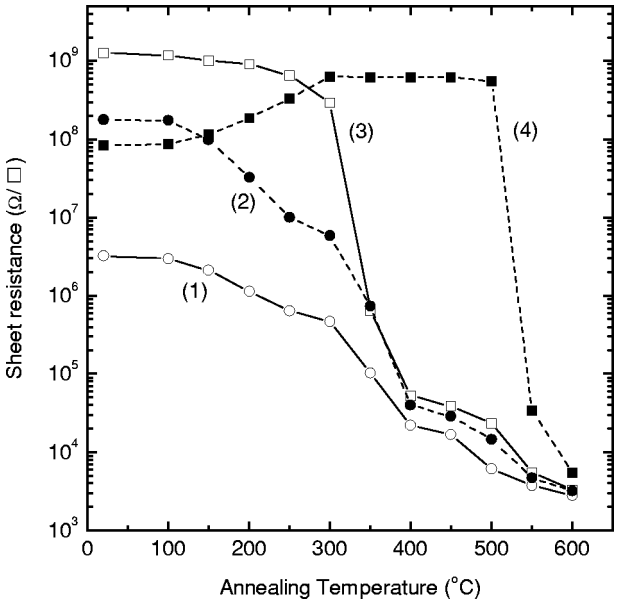

FIG. 5. Evolution of the sheet resistance with the temperature of the postirradiation annealing in samples of structure A after irradiation with protons at the energy of 240 keV. The doses are 2×10^{14} cm^{-2} for curve (1), 2.2×10^{14} cm^{-2} for curve (2), 2.5×10^{14} cm^{-2} for curve (3), and 2×10^{15} cm^{-2} for curve (4).

irradiated to different proton doses at the energy of 240 keV was investigated. The doses were chosen (see Fig. 1) in the leading edge of R_s versus dose curve (2×10^{14} cm^{-2} or 0.8 D_{th} and 2.2×10^{14} cm^{-2} or $0.9D_{\text{th}}$) at the beginning of the plateau (2.5×10^{14} cm^{-2} or D_{th}) and in hopping region of the curve (2×10^{15} cm^{-2} or $8D_{\text{th}}$).

The effects of the postirradiation annealing cycles on R_s are shown in Fig. 5. In the samples irradiated with doses $\leqslant D_{\text{th}}$, four stages of annealing are apparent [see curves (1) and (2) in Fig. 5]. In the temperature range of 20–100 °C there is essentially no variation of R_s. In the temperature range from 100 to 300 °C a monotonic and gradual decrease of R_s ($\approx$1 order of magnitude) is observed. Above 300 °C, a sudden decrease of R_s by 2–4 orders of magnitude occurs. Another annealing stage starts at 400 °C and leads to the restoration of the original R_s value.

In the sample irradiated to D_{th}, the temperature range where the isolation persists is restricted to values below $\approx$300 °C [see curve (3) in Fig. 5]. In the temperature range of 350–400 °C there is an abrupt recovery of R_s by 3–4 orders of magnitude. A second annealing stage in the temperature range of 500–600 °C recovers the original R_s value.

Remarkable enhancement in the isolation stability is observed when the dose is increased to $8D_{\text{th}}$ [see curve (4)]. In the temperature range of 100–300 °C R_s increases monotonically. This behavior results from a progressive annealing of the radiation damage responsible for hopping conduction. Above 300 °C the hopping conduction has been extinguished already and then R_s is maintained at its highest level of $\approx10^9$ Ω/□. However, in the temperature range of 500–600 °C a sharp decrease of R_s occurs with a complete recovery of its original value.

The data plotted in curves (1)–(4) of Fig. 5 clearly indicate that there are two main annealing stages starting at temperatures of $\cong$300 and 500 °C. Considering that P_{In} and P_{Ga} are donor-like antisite defects, their annealing would produce the observed decreasing of R_s, due to the release of the captured holes. One should consider that the P_{In} and P_{Ga} antisite defects have the same first-neighbor structure. Both consist of a P atom connected to four other P atoms by covalent bonds. The existence of two main annealing temperatures very likely suggests that other defect structures are taking place for carrier capture, like for example, antisite related defect complexes.

IV. CONCLUSIONS

The formation of electrical isolation in InGaP/GaAs structure via light mass ion irradiation and the thermal stability of the formed isolation during postirradiation annealing were investigated.

The behavior of R_s during the dose accumulation in InGaP layers is quite similar to those already observed in irradiated GaAs (Ref. 15) and InP.[16] The threshold dose for isolation was found in direct proportion with the original carrier concentration in the InGaP layer, irrespectively of the conduction type of the layer. According to TRIM code simulation and data in Fig. 4 the threshold for isolation is attained when an ion dose, which produces $\cong2\pm0.5$ replacement collisions per carrier in the InGaP layer, is accumulated. Our results suggest that antisite and/or antisite related defect complexes are the carriers trapping centers in InGaP material, similarly to what was inferred for GaAs (Ref. 15) and InP (Ref. 16) materials.

The thermal stability of isolation was found to increase with the irradiation dose. A significant improvement in the thermal stability was obtained in samples irradiated to the dose of $8D_{\text{th}}$. In these samples the isolation is maintained up to 500 °C, which seems adequate for most of the technological applications.

ACKNOWLEDGMENTS

This work was partially supported by Conselho Nacional de Desenvolvimento Científico e Tecnológico (CNPq), Fundação de Amparo à Pesquisa do Estado de São Paulo (FAPESP), and Fundação de Amparo à Pesquisa do Estado do Rio Grande do Sul (FAPERGS).

[1] M. J. Mondry and H. Kroemer, IEEE Electron Device Lett. **EDL-6**, 175 (1985).
[2] N. B. Zvonkov, S. A. Akhlestina, A. V. Ershov, B. N. Zvonkov, G. A. Maksimov, and E. A. Uskova, Quantum Electron. **29**, 217 (1999).
[3] S. J. Pearton, C. R. Abernathy, and F. Ren. *Topics in Growth and Device Processing of III–V Semiconductors* (World Scientific, Singapore, 1996).
[4] S. J. Pearton, Mater. Sci. Rep. **4**, 313 (1990).
[5] S. J. Pearton, J. M. Kuo, F. Ren, A. Katz, and A. P. Perley, Appl. Phys. Lett. **59**, 1467 (1991).
[6] A. Henkel, S. L. Delage, M. A. DiForte-Poisson, H. Blanck, and H. L. Hartnagel, Jpn. J. Appl. Phys., Part 1 **36**, 175 (1997).
[7] A. Y. Polyakov, A. A. Chelnyi, A. V. Govorkov, N. B. Smirnov, A. G. Milnes, S. J. Pearton, R. G. Wilson, A. A. Balmashnov, A. N. Aluev, and A. V. Markov, Solid-State Electron. **38**, 1131 (1995).
[8] H. Strusny, P. Ressel, K. Vogel, and J. Würfl, Nucl. Instrum. Methods Phys. Res. B **112**, 298 (1996).
[9] J. P. de Souza, I. Danilov, and H. Boudinov, J. Appl. Phys. **81**, 650 (1997).
[10] A. Girardot, A. Henkel, S. L. Delage, M. A. DiForte-Poisson, E. Chartier,

D. Floriot, S. Cassette, and P. A. Rolland, Electron. Lett. **35**, 670 (1999).
[11] K. Mochizuki, R. J. Welty, and P. M. Asbeck, Electron. Lett. **36**, 264 (2000).
[12] J. Bettini, M. M. G. de Carvalho, M. A. Cotta, M. A. A. Pudenzi, N. C. Frateschi, A. Silva Filho, L. P. Cardoso, and R. Landers, J. Cryst. Growth **208**, 65 (2000).
[13] J. F. Ziegler, J. P. Biersack, and U. Littmark. *The Stopping and Range of Ions in Solids* (Pergamon, Oxford, 1985), Vol. 1.
[14] R. Bäuerlein, Z. Phys. **176**, 498 (1963).
[15] J. P. de Souza, I. Danilov, and H. Boudinov, Appl. Phys. Lett. **68**, 535 (1996).
[16] H. Boudinov, J. P. de Souza, and C. Jagadish, Nucl. Instrum. Methods Phys. Res. B **175-177**, 235 (2001).